Step-down converter with voltage stabilization for the electric power plant based on hydrogen fuel elements for unmanned aerial vehicles

View the article online for updates and enhancements.

Step-down converter with voltage stabilization for the electric power plant based on hydrogen fuel elements for unmanned aerial vehicles

I Vasyukov, V Puzin and A Pavlenko

Platov South-Russian State Polytechnic University (Novocherkassk Polytechnic Institute), Prosveshcheniya st., 132, Rostov Region, Novocherkassk, 346428, Russian Federation

E-mail: vasuckov@gmail.com, vspuzin@gmail.com, eea.srspu@gmail.com

Abstract. Issues of developing the step-down converter with voltage stabilization for the electric power plant based on fuel elements have been considered. Three options of the power unit implementation are offered: classic step-down converter, mixing circuit on "ideal diodes" and circuit with stage switching. Advantages and disadvantages of the circuits offered are described. The most suitable converter structure with the stabilization circuit is selected. The method of the electric power plant optimization according to the unmanned aerial vehicle maximum flight time has been specified. Design calculation of the power circuit is carried out, numerical model of the device in LTspice software set is proposed. Numerical simulation of the main converter operation modes has been carried out, its characteristics and requirements to the element base obtained. The test sample experimental studies that have been carried out confirmed its efficiency, adequacy of the methods of design calculation and simulation of converter operation modes.

1. Introduction

The most important part of the electric power plant based on fuel elements for unmanned aerial vehicles (UAV) is the multi-functional electrotechnical set, including the energy-saving voltage converter, the monitoring and control system with sensors and actuating units for fuel feed control and waste product exhausting system [1-5]. Operating modes of the fuel elements as parts of the electric power plant are determined by a large number of parameters: pressure, temperature, electric parameters, moisture of gases fed, the change of which provides the instability of the electrotechnical set [6-8]. Changing the fuel element electric parameters has the considerable impact on the power supply system performance. The volt-current curve of the fuel elements stack has the expressed declining nature, and its output voltage can be almost twice lower than the impedance voltage at the load current change [9, 10].

2. Converter structure

The power source structural-functional circuit was proposed based on the above information. As was noted above, the step-down converter is the main part of the power source. In order to optimize the converter heat mode, the synchronous circuit was applied, the structure of which is given in figure 1. To operate the converter, the synchronous PWM controller LTC7801 is used, which additional advantage

is the possibility to operate with the 100% fill factor. For power loss decrease, current feedback is organized with the use of throttle active resistance as the current sensor. The converter output voltage control was performed by changing the voltage on the soft start output LTC7801 via the digital-to-analog converter. The converter output is connected to the load via the "ideal diode" circuit, implemented on the Q3 transistor. This decision was made due to the peculiarities of the micro circuit LTC7801 operation to ensure safe operating of the converter keys. The battery is connected to the load via the Q4 transistor key. This solution allows disconnecting it when the charge is lower than the minimal voltage.

The digital control system is performed on the micro controller STM32F103 and provides the voltage and current control in three power circuit nodes: on the output of the stack of fuel elements (at the converter input), on the battery, on the load (at the power supply output). Based on the current and voltage data, the micro controller program forms the load voltage by setting the required level at the DAC output. Additionally, the control system monitors the temperature inside the stack of fuel elements, controls the valve for disposal of water and discharge gas and, if required, disconnects the battery. In order to control the stack and converter parameters, and their setting, the control system switches on the telemetry model via wireless channel (Bluetooth). Power is supplied to the control system analogue and digital parts via the diode-OR-ring from the fuel element and the battery. This solution makes possible, if required, operation only from the stack of fuel elements without using the battery. The stack fans are connected to the separate voltage converter at the power source output.
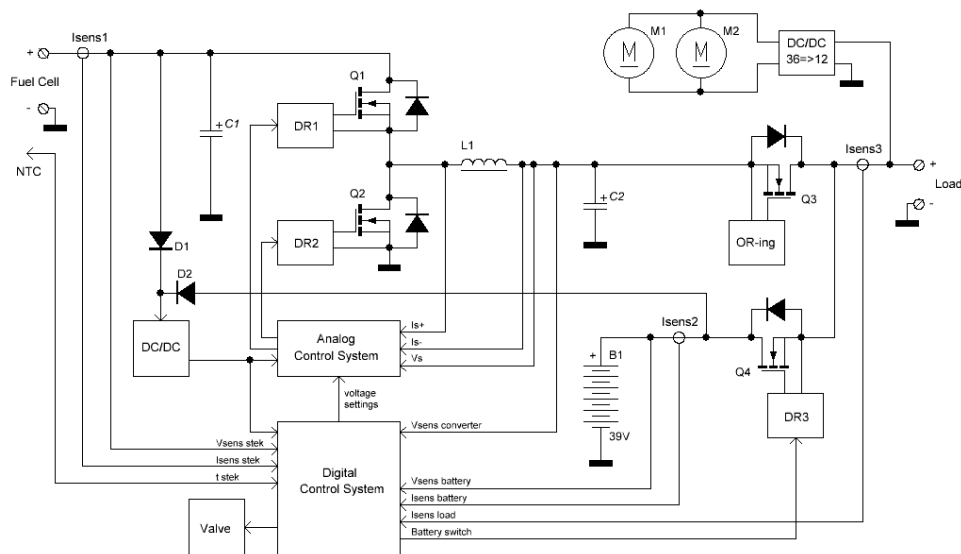

Figure 1. Power source operating diagram.

The step-down converter calculation method was developed for the preliminary selection of the power circuit elements. As the step-down-converter principle of operation is similar to that of the output stage of the bridge converter with hard switch-over, the output of design ratio was carried out similar to that given in [11-14]. The difference is that this circuit has no pulse transformer and, respectively, the value of its stray inductance is excluded from calculation formulas. Parameters obtained in the general form as the result of calculations are given below.

1. Output voltage:

$$U_{out\_over\_stab} = f\left(U_2, U_{vd}, U_{vt}, L, R_{load}, \gamma_f, T_f, I_{over}, I_{out\_avg}, U_{out\_avg}\right),$$

where U_2 – input voltage of the step-down stabilizer,
U_{vd} – voltage drop at the reverse diode,
U_{vt} – voltage drop at the power key,

L – throttle inductivity,

R_{load} – load resistance,

γ_f – PWM fill factor,

T_f – PWM period,

I_{over} – setting of cycle-by-cycle current limiting,

I_{out_avg} – stabilization setting under the output circuit mean value,

U_{out_avg} – setting under the mean output voltage.

2. Load current:

$$I_{out\_over\_stab} = f\left(U_2, U_{vd}, U_{vt}, L, R_{load}, \gamma_f, T_f, I_{over}, I_{out\_avg}, U_{out\_avg}\right).$$

3. Load power:

$$P_{out\_over\_stab} = f\left(U_2, U_{vd}, U_{vt}, L, R_{load}, \gamma_f, T_f, I_{over}, I_{out\_avg}, U_{out\_avg}\right).$$

4. Throttle current amplitude:

$$I_{max\_over\_stab} = f\left(U_2, U_{vd}, U_{vt}, L, R_{load}, \gamma_f, T_f, I_{over}, I_{out\_avg}, U_{out\_avg}\right).$$

5. Throttle current swing:

$$\Delta I_{L\_over\_stab} = f\left(U_2, U_{vd}, U_{vt}, L, R_{load}, \gamma_f, T_f, I_{over}, I_{out\_avg}, U_{out\_avg}\right).$$

6. PWM real fill factor:

$$\gamma_{f\_over\_stab} = f\left(U_2, U_{vd}, U_{vt}, L, R_{load}, \gamma_f, T_f, I_{over}, I_{out\_avg}, U_{out\_avg}\right).$$

7. Throttle effective current:

$$I_{rms\_L\_over\_stab} = f\left(U_2, U_{vd}, U_{vt}, L, R_{load}, \gamma_f, T_f, I_{over}, I_{out\_avg}, U_{out\_avg}\right).$$

8. Key effective current:

$$I_{rms\_VT\_over\_stab} = f\left(U_2, U_{vd}, U_{vt}, L, R_{load}, \gamma_f, T_f, I_{over}, I_{out\_avg}, U_{out\_avg}\right).$$

9. Reverse diode effective current:

$$I_{rms\_VD\_over\_stab} = f\left(U_2, U_{vd}, U_{vt}, L, R_{load}, \gamma_f, T_f, I_{over}, I_{out\_avg}, U_{out\_avg}\right).$$

10. Converter performance factor:

$$\eta_{over\_stab} = f\left(U_2, U_{vd}, U_{vt}, L, R_{load}, \gamma_f, T_f, I_{over}, I_{out\_avg}, U_{out\_avg}, R_{vt}, R_{vd}, R_L\right),$$

where R_{vt} is the key active resistance,

R_{vd} – reverse diode active resistance,

R_L – throttle active resistance.

11. Induction range in the throttle magnetic core:

$$\Delta B_{over\_stab} = f\left(U_2, U_{vd}, U_{vt}, L, R_{load}, \gamma_f, T_f, I_{over}, A_e, w, I_{out\_avg}, U_{out\_avg}\right),$$

where A_e – throttle, magnetic core section,

w – number of throttle coils.

12. Maximal value of induction in the throttle magnetic core:

$$\Delta B_{\max\_over\_stab} = f\left(U_2, U_{vd}, U_{vt}, L, R_{load}, \gamma_f, T_f, I_{over}, A_e, w, I_{out\_avg}, U_{out\_avg}\right).$$

Calculation formulas allow obtaining surfaces of parameters of interest in order to define their maximal values, corresponding to the most severe conditions of elements operation. The preliminary selection of elements of the converter power unit is carried out by maximum values. The calculation method proposed can be used as a component for solving the issue of optimization under the maximum flight

time of the unmanned aerial vehicle with the electric power plant based on hydrogen fuel elements. The main design ratios for such optimization were proposed in [15], but the converter weight $m_{converter}$ and its performance factor $\eta_{converter}$ were admitted constant for simplification. The converter weight assessment can be carried out by calculating parameters for the most severe converter conditions, according to the method proposed. While calculating the electric power plant performance factor, converter losses can also be taken into account with the higher accuracy. As the result, the final calculation formula for the electric power plant optimization according to the flight time will have the following form:

$$t_{flight}(U,n) = \frac{E_{fuel} \cdot \eta_{STAK} \cdot \eta_{converter}(U,n)}{P_{STAK}(U,n)}.$$

At this, the electric power plant weight at each iteration is defined as:

$$m_{ps} = m_{STAK}(U,n) + m_{converter}(U,n) + m_{battery} + m_{ballon}.$$

During the UAV maneuvers, it can momentary consume extra power which can not be provided by the fuel element. To solve this issue, it is reasonable to use the dedicated voltage stabilization circuits. The stabilization circuit can solve this issue due to adding power from a smaller battery at the peak load moments and by recharging it for the rest of time, thus causing the highest impact at the specific characteristics of the entire electric power plant based on hydrogen fuel elements.

As the example, let us consider the electric power plant of kilowatt power rating with the permissible voltage change range from +10% to -10% of nominal voltage, maximal 50% overload from nominal output voltage during 2 minutes and pauses between the power peaks of about 40 min, defined by the flight mode.

In order to meet the overload requirements, the power accumulator should be used, because FE will not be fully loaded in the nominal operation mode. An accumulating mechanism should generate high pulse currents for the short time intervals. Such accumulating mechanisms as condensers have small capacity. Ionistors (supercapacitors) have unsatisfactory weight-size parameters - 5...6 W·h/kg [16, 17]. Reasoning from this fact, a li-polymer battery able to generate high current discharges was selected.

3. Circuit Solutions
Circuit solutions for the options of implementing the power part of stabilizing scheme is given in figure 2.
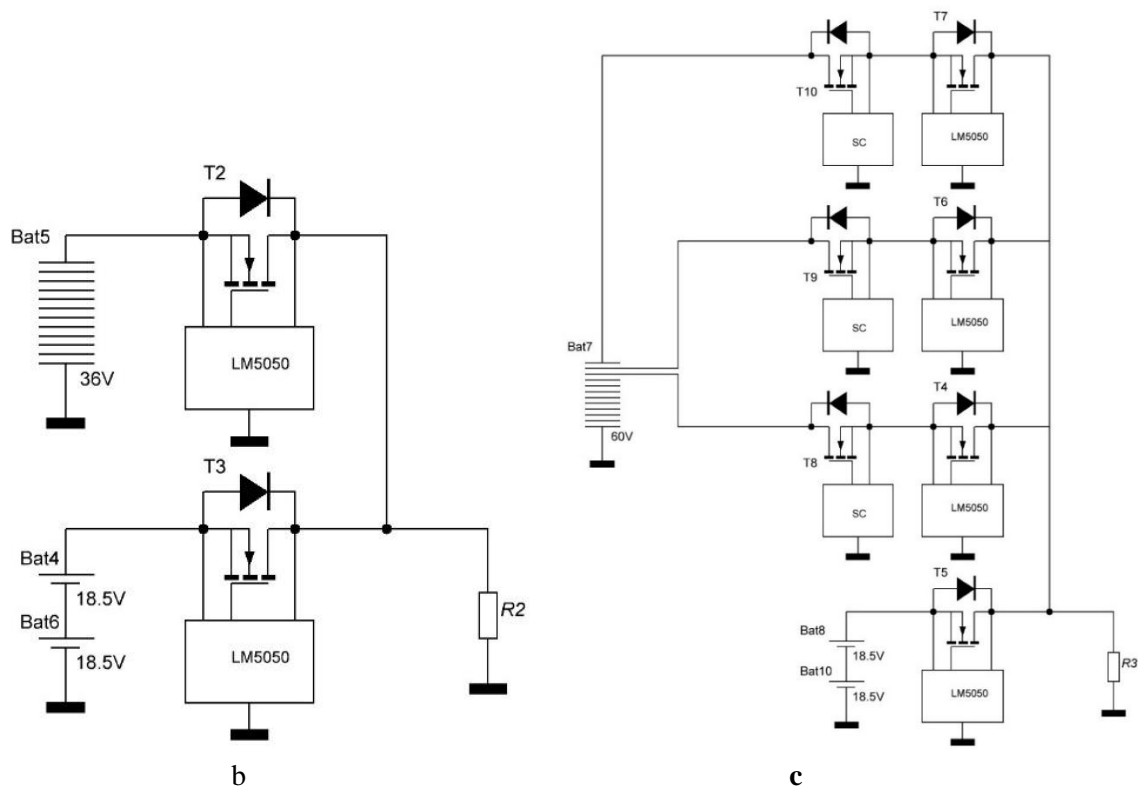

a
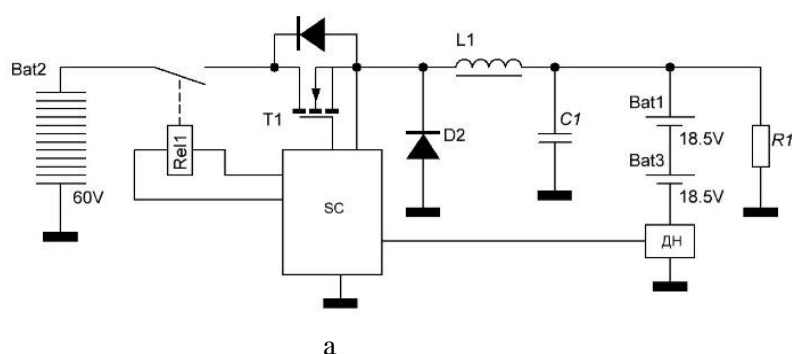
Figure 2. Options of the voltage stabilizer implementation: (a) is a classic step-down pulse converter with a battery connected in parallel to the load, (b) is represented by the diode-OR-ring, (c) switchable circuit

Option 1 is a classic step-down pulse converter with a battery connected in parallel to the load. The reason for selecting the step-down converter is that, in distinction from the other devices, it can operate at the respective selection of elements with 100% filling at maximal load. The system controls the accumulator charge current in the process of operation due to the output voltage management. In this circuit, while the electric power plant is stopped, it is required to disconnect either the battery, or the fuel element, because voltage can be fed to the stack without hydrogen and, as a consequence, its damage is possible through the power key reverse diode. For the fuel element protection, the relay was included into the circuit.

Option 2 is represented by the diode-OR-ring. For losses decrease, MOSFET transistors, controlled by dedicated micro circuits, are used instead of the diodes. Under this technical solution, an impedanve output voltage will correspond to the highest voltage from both sources. At maximal load, both voltage sources are switched into operation, in accordance with their volt-current curves. The disadvantage of this circuit is the missing possibility to adjust the output voltage and its considerable variation range during the operation.

Option 3. As the fuel element stack is a large number of series-connected membrane electrode assemblies with the operating voltage of 1...0,6 V, it is reasonable to use with no-load only part of them to provide the set output voltage. At this, the elements not used will not consume hydrogen. Therefore, by switching lead-outs from the stack, it is possible to support output voltage in the set range. In order to provide the best performance of the circuit, it is required to use semi-conductor keys, in particular, MOSFET transistors, that have the in-built reverse diode as their part. In this case, when opening any lead-out key, the part of membrane electrode assemblies can be short-closed via reverse diodes of the other keys, that will cause the plant failure. Ideal diodes, proposed in the option 2, were added to the circuit with the purpose to avoid this problem. Moreover, similar to option 2, the battery was introduced

in the circuit via the diode-OR-ring. At this, due to exclusion of PWM-transformation, losses in the throttle and in condensers, the possibility appears to decrease total losses in the electric power plant.

Figure 3 shows the VAC of the 70-cell fuel element stack, limits of the permissible output voltage and the external characteristics of the stabilization circuit with four lead-outs, including lead-outs with maximal voltage. As seen in the figure, the first lead-out key can be selected for the lower current - around 2A, for the next lead-out - for 15A, and for the last two higher than the maximum assembly current - around 45A.
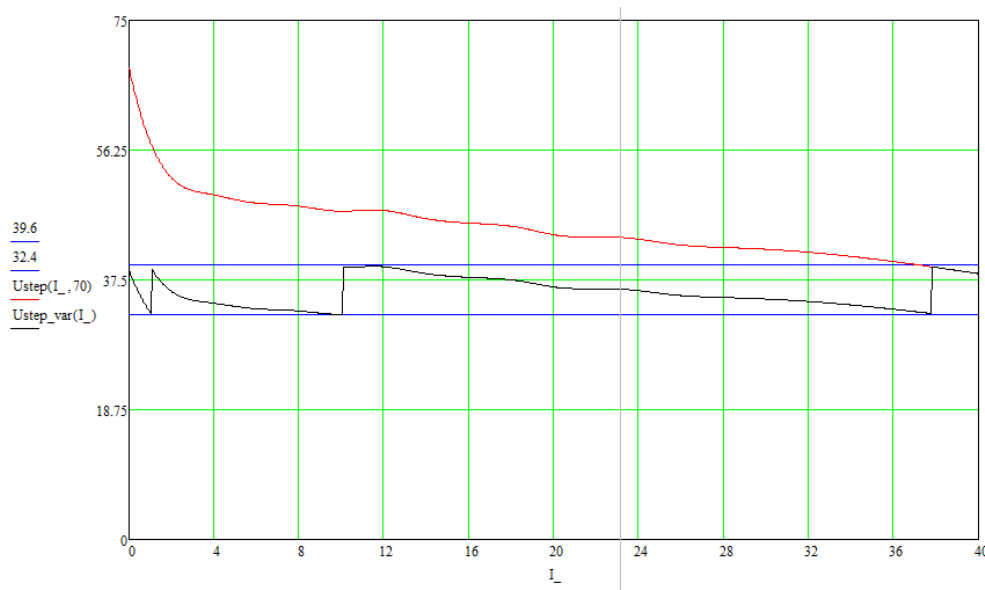

Figure 3. VAC of the 70-element stack and external characteristic of the voltage stabilizer with switchable lead-outs. The corridor of the output voltage permissible values is shown with straight lines.

The first option advantage is the output voltage maintenance accuracy, ease of its adjustment, lower capacity and, respectively, weight of the buffer battery. Disadvantages: system complexity, high losses due to dynamic key loss, the need for the opening key at the fuel element or the battery output with the purpose to exclude the situation with the high voltage supply from the battery to the FE with a lower impedance voltage at this moment. The second option is the simplest in its design, although, it has an underutilization of the fuel element specific capacity, as for the efficient up-mixing of power from the battery, the FE must operate in a mode far from critical. At this, the accumulator power should be uprated, because its recharge is missing in this circuit. In addition, the too wide variation range of the output voltage from no-load to nominal load, not suitable to the most consumers, is provided here. The third option of the stabilization circuit, with its comparative simplicity, has almost zero dynamic loss for switching, because their frequency is minimal, so the possibility to adjust the output voltage appears. The main disadvantages of the scheme are: decrease of specific performance of the part of membrane electrode assemblies at a part-load operation, the need to perform lead-outs from membrane electrode assemblies, the increase of number of semi-conductor keys and, consequently, the circuit cost increase.

The analysis of advantages and disadvantages of the options considered demonstrated that the first circuit option was the most promising due to the provision of wide adjustment of output voltage, protection, and the highest launch speed.

4. Mathematical model

In order to check the completeness of the converter power unit design calculation performed above, a model in the LTspice IV application (figure 4) was developed for the analysis of processes in the

converter. The model included a fuel element, a step-down converter with a fixed transformation frequency, and a resistive load. The fuel element was represented as the idling stack EMF from 75 cells and the internal resistance [18, 19]. Assembly inductivity was simulated by the element L2.
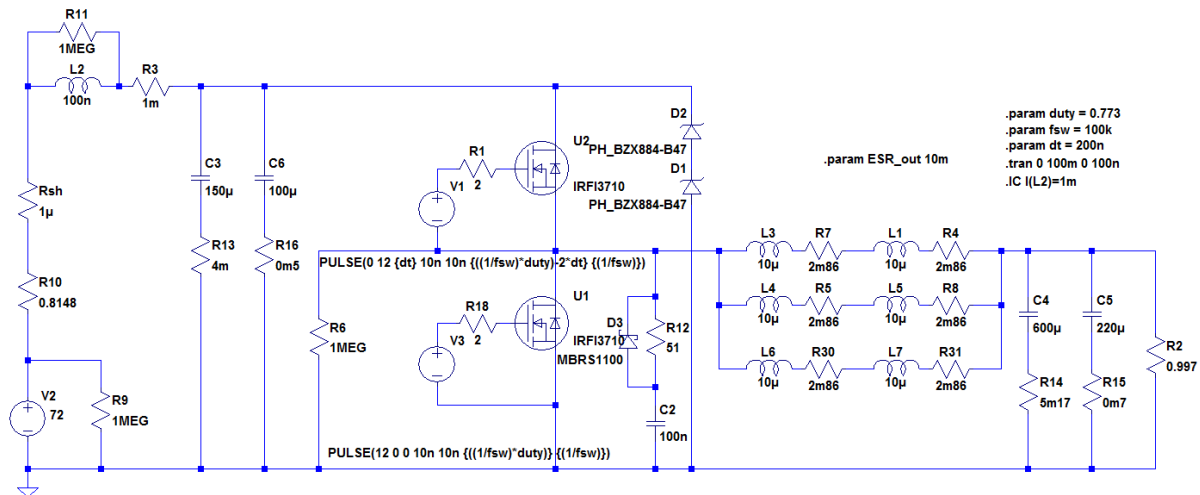

Figure 4. 1300 W Converter model.

Parameters of the converter condensers and throttles were set in accordance with the manufacturer's data. The synchronous step-down converter operated at the frequency of 100 kHz, with pauses between intervals of controlled keys conductivity of 200 ns and the filling coefficient of 0,773. The results of the converter simulation in the mode set are shown on figures 5-8 and in table 1. Output voltage of the converter (figure 5) has the ripple range matching to the given one. Pulse form of the fuel element output current (figure 6, 7) contributes to its moisturing and, to the certain extent, compensates for the absence of periodic short circuits [20]. Under the throttle current oscillogram (figure 8), the maximal current calculated value was clarified, and the required amount of serial/parallel throttles, able to operate in linear mode at this current value, was selected.

Table 1. Simulation results.

| Parameter	Value
Output voltage (mean value), V	36.01
Output voltage ripple range, V	0.042
Output voltage ripple ratio, %	0.06
FE output voltage (mean value), V	49.56
FE output voltage ripple range, V	0.348
FE output current (mean value), A	27.47
FE output current ripple range, A	0.4
Power released in FE, W	614.8
Throttle assembly current (mean square value), A	36.35
Throttle assembly current range, A	14.12
Max. throttle assembly current, A	43.11
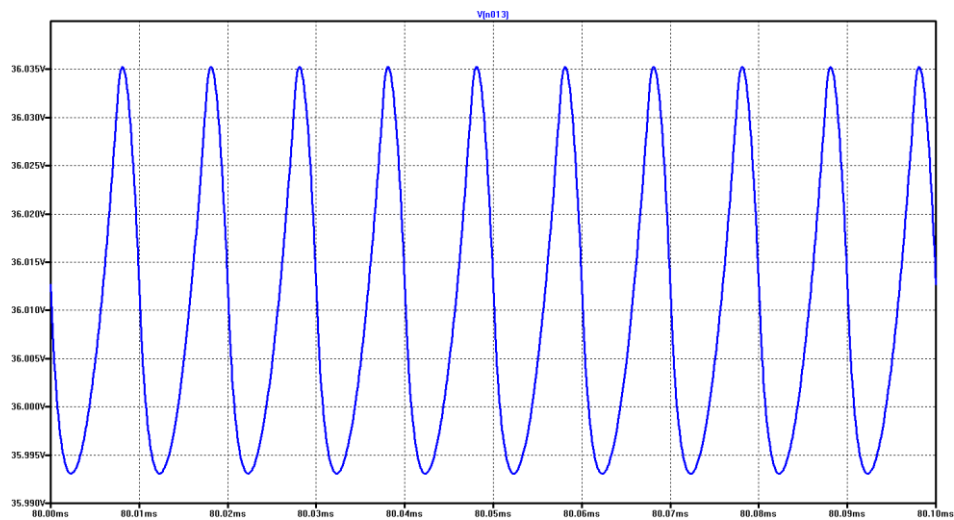
Figure 5. Output voltage of the converter.
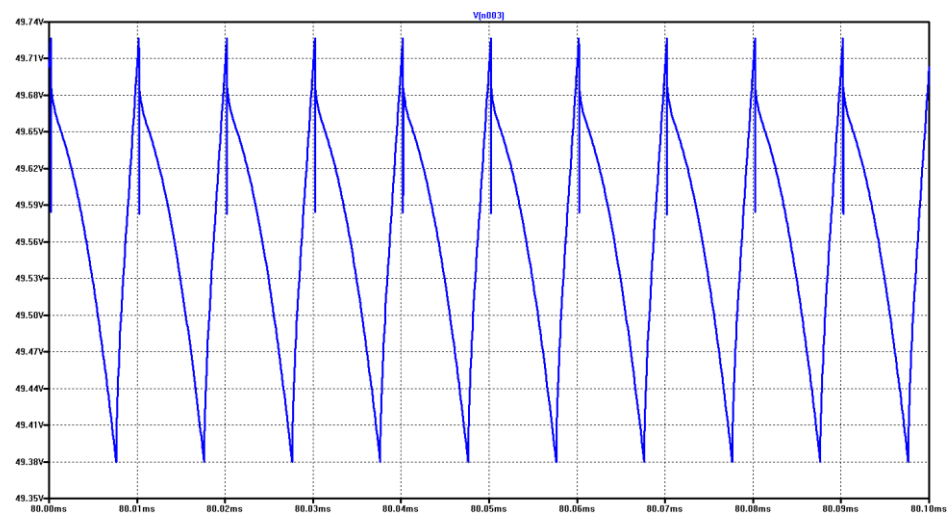

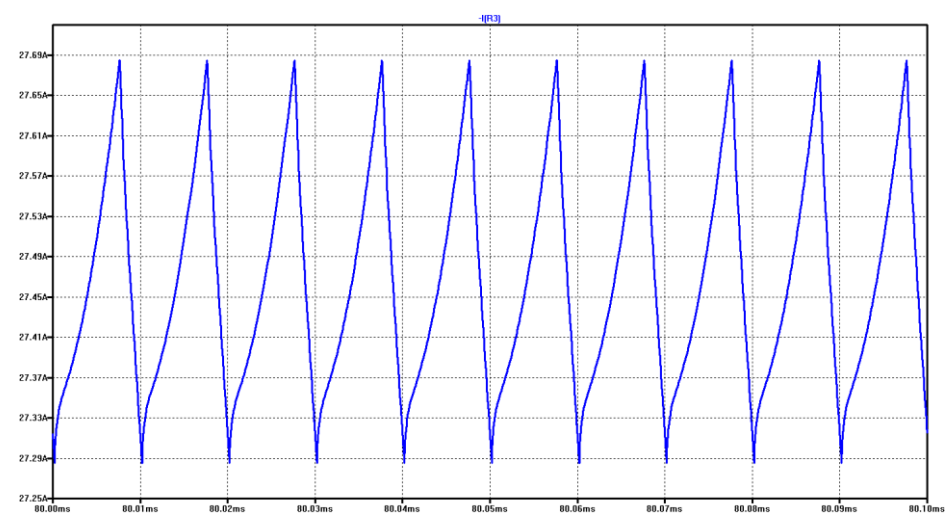**Figure 6.** Output voltage of the fuel element

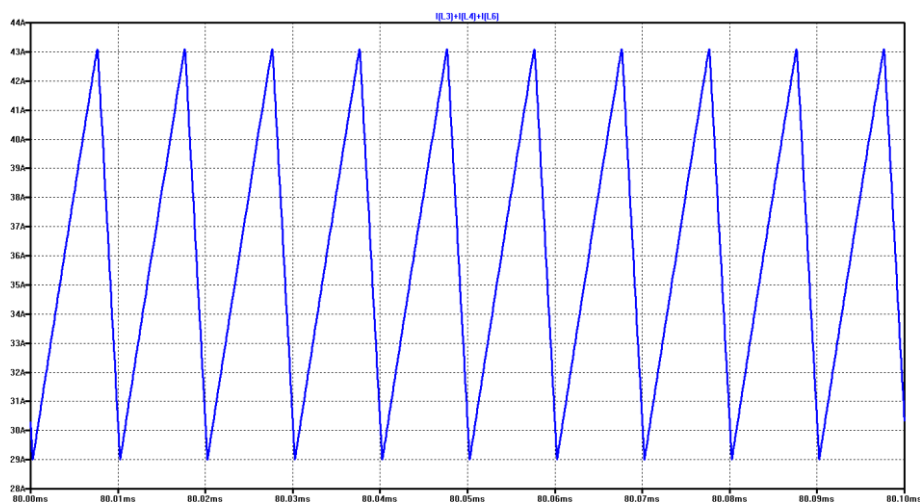**Figure 7.** Output current of the fuel element.

Figure 8. Throttle assembly current.

5.   Experimental research

Based on the design calculation performed and simulation of the main operation modes, the converter experimental sample was made, and its tests were carried out. At the initial test stage, the electronic load, allowing to maintain the energy input of 1300 W, was connected to the converter output. The tests demonstrated the electric power plant conformity to the technical requirements given. At this, output voltage was adjusted in the range from 32 to 39 V, output capacity was maintained at the level of 1300 W with short reloads to 2000W during 2 minutes. Throttles were operating under normal conditions without saturation. Figure 9 shows the application window with the telemetry of the experimental converter parameters: voltage and current of the converter, voltages and currents of the stack of fuel elements and the battery in the set mode.
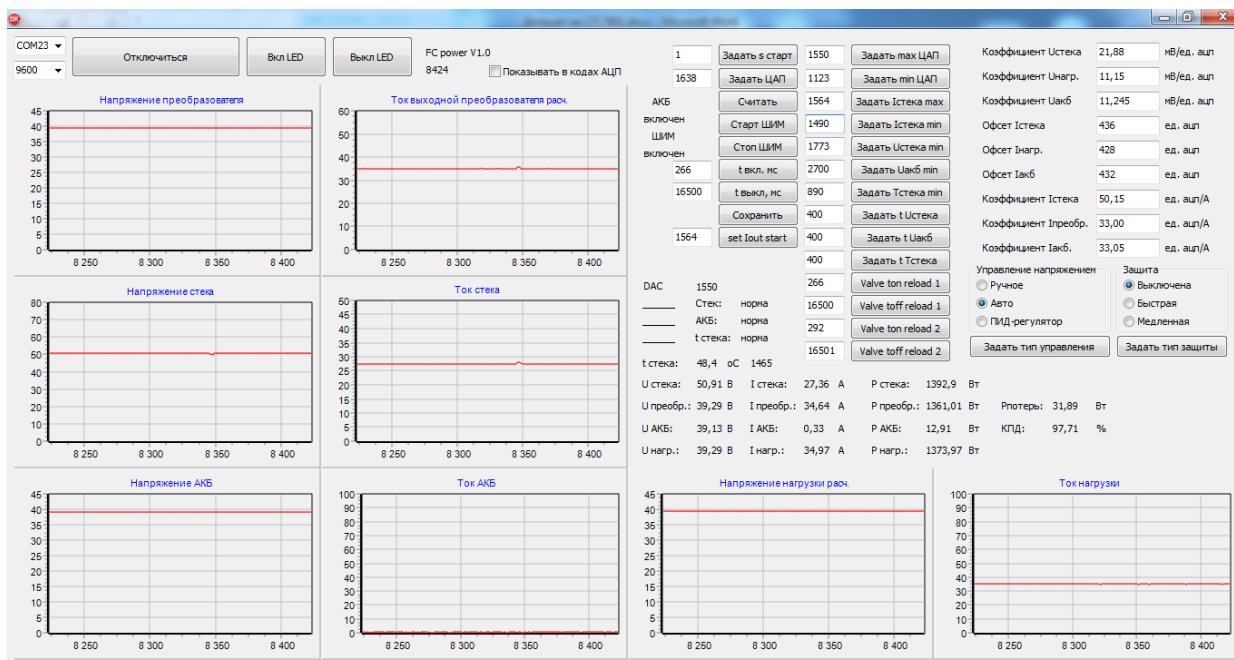

Figure 9. Experimental data. Voltage and current values in control points are indicated at the Y axis. Reading ordinal number is indicated at the X axis.

On the stack voltage graph, a slight dip, corresponding to the moment of opening the valve for disposal of water and impurities accumulated in water, can be seen. At the arrangement, by varying the period and the duration of the valve opened condition, it was required to achieve the minimal value of this dip, and fast recovery.

6.   Conclusion

In sum, the structure and design of the step-down converter for the UAV electric power plant on hydrogen fuel elements were proposed, based on the investigation carried out. The test sample experimental studies that have been carried out confirmed its efficiency, adequacy of the methods of design calculation and simulation of converter operation modes.

Acknowledgments

References

[1]   European Commission EUR 20719 EN – Hydrogen Energy and Fuel Cells – A vision of our future // Luxembourg: Office for Official Publications of the European Communities 2003 - 36 pp. - 21 x 29,7 cm, ISBN 92-894-5589-6

[2]   Fuel Cell and Battery Electric Vehicles Compared By C. E. (Sandy) Thomas, Ph.D., President H2Gen Innovations, Inc. Alexandria, Virginia Thomas@h2gen.com: https://www.energy.gov/sites/prod/files/2014/03/f9/thomas_fcev_vs_battery_evs.pdf

[3]   Hydrogen Fuel Cells for Small Unmanned Air Vehicles // https://www.energy.gov/sites/prod/files/2016/05/f32/fcto_webinarslides_h2_fc_small_unma nned_air_vehicles_052616.pdf

[4]   Brian Cook 201 *An introduction to fuel cells and hydrogen technology* (Canada: Heliocentris 3652 West 5th Avenue Vancouver, BC V6R-1S2)

[5]   Eric Dickinson, Erik Klinkhamer, Gawain Thomas and Rachel Winsten The Future of Fuel Cells in Australia *An Interactive Qualifying Project, WORCESTER POLYTECHNIC INSTITUTE*

[6]   Federico Zenith 2007 Control of fuel cells *Doctoral thesis for the degree of philosophiæ doctor Trondheim Norwegian University of Science and Technology Faculty of Natural Sciences and Technology Department of Chemical Engineering*

[7]   Richard Rios, Carlos A. Ramos-Paja and Jairo J Espinosa 2016 A control systems for reducing the hydrogen consumtion of PEM fuel cells under parametric uncertainties *Tecno Lógicas* **19(37)** 0123-7799 pp. 45-59

[8]   Setareh Shahsavari 2011 Thermal Analysis Of Air-Cooled Fuel Cells, Master Of Applied Science *In the School of Engineering Science Faculty of Applied Sciences Setareh Shahsavari* SIMON FRASER UNIVERSITY

[9]   Roy F, Poirot J P and Garnit S 2009 FiSyPAC project: The first vehicle integration of GENEPAC fuel cell stack *World Electric Vehicle Journal* **3** 2032-6653

[10]   Hubert A. Gasteiger, Daniel R. Baker, Robert N. Carter, Wenbin Gu, Yuxin Liu, Frederick T. Wagner, and Paul T. Yu 2010 Electrocatalysis and Catalyst Degradation Challenges in Proton Exchange Membrane Fuel Cells *Hydrogen Energy. Edited by Detlef Stolten Copyright © 2010 WILEY-VCH Verlag GmbH & Co. KGaA Weinheim* 978-3- 527-32711-9

[11]   Pavlenko A V, Puzin V S and Vasyukov I V 2014 Design of the output filter of a high-voltage switching power supply *Izv. Universities.Electromechanics* **1** 58-62

[12]   Pavlenko A V, Vasyukov I V, Puzin V S, Grinchenkov V P and Bol'shenko A V 2015 Designing of the Output Stage of the Impulse Power Source *Russian Electrical Engineering* **8** 453-8

[13]   Bolshenko A V, Pavlenko A V and Vasyukov I V 2016 Output Filter Designing for Power

Supplies Considering Leakage Inductance Industrial Engineering *Applications and Manufacturing (ICIEAM), International Conference on IEEE* DOI: 10.1109/ICIEAM.2016.7911507

[14] Pavlenko A V, Puzin V S, Vasyukov I V, Zhivodernikov A V, Batyukov A V and Shcherbakov A V 2018 Calculation of the External Characteristic of a Switched-Mode Power Supply X *International Conference on Electrical Power Drive Systems (ICEPDS)* DOI: 10.1109/icepds.2018.8571828

[15] Vasyukov I V, Faddeev N A, Kramarov A S, Gummel A A, Puzin V S and Batyukov A V 2019 Power installation of an unmanned air vehicle based on a hydrogen fuel cell *2019 26th International Workshop on Electric Drives: Improvement in Efficiency of Electric Drives (IWED) IEEE*

[16] Obreja V V N 2007 On the Performance of Commercial Supercapacitors as Storage Devices for Renewable Electrical Energy Sources *International Conference on Renewable Energy and Power Quality (ICREPQ2007)*

[17] Yao Y Y, Zhang D L and Xu D G 2006 A Study of Supercapacitor Parameters and Characteristics *International Conference on Power System Technology* DOI: 10.1109/ICPST.2006.321487

[18] Zehra Ural 2010 Muhsin Tunay Gencoglu, Mathematical Models of PEM Fuel Cells *5th International Ege Energy Symposium and Exhibition (IEESE-5)*

[19] Thomas Strele 2016 Power Management for Fuel Cell and Battery Hybrid Unmanned Aerial Vehicle Applications *Master Thesis Arisona State University*

[20] H-20 Fuel Cell Stack, User Manual, 13 Dec. 2011: https://www.fuelcellstore.com/manuals/horizon-pem-fuel-cell-h-20-manual.pdf.